Deep–Sea Research Part I 122 (2017) 81–94

Contents lists available at ScienceDirect

Deep–Sea Research I

journal homepage: www.elsevier.com/locate/dsri

Dynamic benthic megafaunal communities: Assessing temporal variations in structure, composition and diversity at the Arctic deep-sea observatory HAUSGARTEN between 2004 and 2015

J. Taylor*, T. Krumpen, T. Soltwedel, J. Gutt, M. Bergmann

Alfred-Wegener-Institut, Helmholtz-Zentrum für Polar- und Meeresforschung, Am Handelshafen 12, D-27570 Bremerhaven, Germany

ARTICLE INFO

Keywords:
Arctic
Deep sea
Image analysis
Epibenthic megafauna
Long-term ecological research
Photo/video system
Time series

ABSTRACT

Established in the Fram Strait in 1999, the LTER (Long-Term Ecological Research) observatory HAUSGARTEN enables us to study ecological changes on the deep Arctic seafloor. Repeated deployments of a towed camera system (Ocean Floor Observation System) along the same tracks allowed us to build a time series longer than a decade (2004–2015). Here, we present the first time-series results from a northern and the southernmost station of the observatory (N3 and S3, ~2650 m and 2350 m depth respectively) obtained via the analysis of still imagery. We assess temporal variability in community structure, megafaunal densities and diversity, and use a range of biotic factors, environmental sediment parameters and habitat features to explain the patterns observed. There were significant temporal differences in megafaunal abundances, diversity and habitat features at both stations. A particularly high increase in megafaunal abundance was recorded at N3 from 12.08 (± 0.39; 2004) individuals m^{-2} to 35.21 (± 0.97; 2007) ind. m^{-2} alongside a ten-fold increase in (drop-)stones. At S3, megafaunal densities peaked in 2015 (22.74 ± 0.61 ind. m^{-2}) following a general increase since 2004 (12.44 ± 0.32 ind. m^{-2}). Sea cucumbers showed particularly striking temporal differences: densities of the small holothurian *Elpidia heckeri* rose ten-fold from 0.31 ind. m^{-2} (± 0.04; 2004) to 3.74 ind. m^{-2} (± 0.14; 2015) at S3, and 24-fold from 0.09 ind. m^{-2} (± 0.02; 2004) to 2.20 ind. m^{-2} (± 0.10; 2015). Initially entirely absent from N3, densities of the larger holothurian *Kolga hyalina* peaked in 2007 (5.87 ± 0.22 ind. m^{-2}) and declined continuously since then. Overall diversity (γ) increased at both stations over the course of the study, however, with varying contributions of α and β diversities.

Our results highlight the importance of time-series studies as megafaunal community structure is characterised by continuous changes. This indicates that epibenthic communities from the deep seafloor are reactive and dynamic, with no consistent community state. To continue to monitor them is therefore crucial in understanding natural and anthropogenic impacts in an area exposed to the effects of climate change.

1. Introduction

Time-series studies allow us to follow changes in deep-sea benthic communities in detail and to identify the key drivers of such ecosystems. However, studies that extend for periods longer than a decade are generally rare and only a handful exist for megafauna, defined here as organisms > 1.5 cm in length (Grassle et al., 1975; Rex, 1981). This is predominantly down to technological and logistical constraints, especially in the Arctic Ocean. Long-term studies have been conducted at Station M, in the northeast Pacific (e.g. Lauerman et al., 1996; Ruhl, 2007) and the Porcupine Abyssal Plain (PAP) (e.g. Billett et al., 2001; Billett et al., 2010), both locations showing significant temporal variability in epibenthic megafaunal communities. At the HAUSGARTEN observatory, interannual changes in the megafaunal communities have been previously studied for stations HG-IV (2500 m) and HG-I (1200 m), over a period of five and ten years respectively (Bergmann et al., 2011; Meyer et al., 2013). Epibenthic organisms perform as ecosystem engineers (Jones et al., 1994), continually sculpting their habitats, with mobile megafauna creating tracks and burrows. Sessile megafauna increase habitat complexity through biogenic structures, creating potential for a greater diversity of smaller infauna, hard substrata for epibionts and possible shelter or protection from predation (Buhl-Mortensen et al., 2010; Meyer et al., 2014). Perhaps the most important role for epibenthic megafauna is

* Corresponding author.
E-mail addresses: James.Taylor@awi.de (J. Taylor), Thomas.Krumpen@awi.de (T. Krumpen), Thomas.Soltwedel@awi.de (T. Soltwedel), Julian.Gutt@awi.de (J. Gutt), Melanie.Bergmann@awi.de (M. Bergmann).

http://dx.doi.org/10.1016/j.dsr.2017.02.008
Received 4 August 2016; Received in revised form 1 February 2017; Accepted 23 February 2017
Available online 01 March 2017

the one they play in the global carbon cycle, with the redistribution of oxygen and organic and nutritional matter in the surface sediments via bioturbation, oxygenation and remineralisation (Buhl-Mortensen et al., 2015). Time-series studies allow for greater understanding of this key role and how it affects the world's largest carbon sink (Bett et al., 2001; Ruhl, 2007; Fitz-George-Balfour et al., 2010).

Arctic sea ice is declining at rates greater than previously suggested in model projections (Kauker et al., 2009), such that the Arctic may potentially become ice-free within this century (Wang and Overland, 2009). Already this results in a retreat of the ice edge and loss of multi-year ice, and may lead to a lower flux of fast-sinking ice algae and ice-associated particulate organic matter in the long run (Gutt, 1995; Hop et al., 2006; Boetius et al., 2013). A decreased deposition of vital nutrients to the deep seafloor, an environment already characterised by food limitation (Smith et al., 2008), could alter benthic community structure.

Here, we assess temporal variations in the epibenthic megafaunal community through analysis of seafloor photographs from two stations (N3 and S3) spanning a period of 11 years. The study of a primarily ice covered and an ice-free station potentially enables us to observe how each community changes over time, as well as giving us a glimpse of the potential future of more northern epibenthic communities after the retreat of sea ice. The specific questions addressed in this study are: (1) do either of the stations (N3 and S3) display temporal variations in megafaunal density or community structure over the study period? (2) If there are temporal variations, what are the factors driving these variations? (3) How does diversity vary over the course of the study and what does this tell us about the community? We discuss these in terms of environmental sediment parameters, sea-ice coverage and habitat features.

2. Material and methods

2.1. Study location

Established in 1999, the LTER (Long-Term Ecological Research) observatory HAUSGARTEN currently comprises 21 sampling stations along a bathymetric and latitudinal gradient in the Fram Strait (Soltwedel et al., 2016). The Fram Strait is the only connection for the exchange of deep and intermediate water masses between the north Atlantic and central Arctic Ocean (von Appen et al., 2015), with the hydrography of the studied sites characterised by the inflow of relatively warm, nutrient-rich water leading to the central Arctic Ocean (Beszczynska-Möller et al., 2012). Our study focuses on a northern (N3) and on the southernmost (S3) station of the observatory, which are part of the latitudinal transect that was targeted to run along the 2500-m isobath as based on data from the General Bathymetric Chart of the Oceans (GEBCO) (Fig. 1). Since establishment the AWI has been able to perform more detailed bathymetric mapping of the area and station N3 turned out to be approximately 300–400 m deeper than S3. However, due to a similar species composition at both stations, with depth ranges of observed species encompassing both stations, they are considered two comparable communities (Taylor et al., 2016). The station S3 remains mostly ice free over the course of the year whilst station N3 experiences ice coverage. Melting of this sea ice in spring and summer contributes to a stratified Marginal Ice Zone (MIZ), which is nutrient rich, causing intense phytoplankton blooms and regionally enhanced fluxes of particulate organic matter (Bauerfeind et al., 2009; Lalande et al., 2013). Consistent annual sampling campaigns and deployments of long-term moorings and free-falling systems have yielded a comprehensive data set comprising faunal, bacterial and biogeochemical data, as well as geological properties and hydrography and sedimentation patterns, allowing for a greater potential understanding of the wide variety of linked systems and the factors contributing to their changes (Bauerfeind et al., 2009; Forest et al., 2010; Hasemann and Soltwedel, 2011; Jacob et al., 2013; von Appen et al., 2015; Soltwedel et al., 2016).

2.2. OFOS specifications and deployment

In 2004 and 2007, an analogue Ocean Floor Observation System (OFOS) was chartered from Oktopus, Germany. As of 2011, the Alfred Wegener Institute (AWI) has used its own digital OFOS, which has been continually upgraded. This has resulted in different OFOS configurations all of which included a still camera mounted onto the steel frame positioned perpendicular to the seafloor (Table 1), an altimeter and telemetry was added in 2013.

Seafloor images of the two transect stations analysed during this study were obtained during the expeditions ARK-XX/1 (2004), ARK-XXII/1 (2007), ARK-VI/2 (2011), ARK-XXVII/2 (2012), ARK-XXVIII/1 (2014) and ARK-XXIX/2 (2015) aboard the German icebreaker *Polarstern* and MSM29 (2013) aboard RV *Maria S. Merian*.

The OFOS was towed at each station for four hours at ~0.5 knots to cover a distance of 4 km at a target altitude of 1.5 m. The altitude was controlled, under instruction, by a winch operator, reacting to variations in seafloor topography and sea state to maintain the target altitude. The still camera was triggered automatically at 30-second intervals to avoid spatial overlap of images and replication of features. Table 2 gives the details of all OFOS deployments.

2.3. Image selection and analysis

All images in a transect were sorted by a random number and subject to a quality check (Taylor et al., 2016). The first 80 images, which covered between 3.5 and 4.5 m^2 in area, were selected for the study. This process was done for every year, at both stations.

The images were analysed in the web- 2.0 based platform BIIGLE (Benthic Image Indexing and Graphical Labelling Environment) (Ontrup et al., 2009). Each image was labelled by the same taxonomic expert twice, to even out learning effects, at maximum zoom. Upon completion, an “area box” was placed on the image, removing labels in dark or potentially slightly blurred areas to improve the accuracy of density estimates. The three laser points (two in 2007) present in each image were detected by a computer algorithm (Schoening et al., 2015) and used as a standard to calculate the area of the “area box”, allowing the conversion of individual counts to densities. All analyses were conducted in a shaded room, to reduce external glare. The same computer/monitor set up was used in all analyses to remove variation brought about by varying resolution.

2.4. Sea-ice data and seafloor environmental sediment parameters

To obtain information about sea-ice conditions, daily sea-ice concentration data were extracted over the positions of the two stations. Data were obtained from the Center for Satellite Exploitation and Research (CERSAT) at the Institut Français de Recherche pour l’Exploitation de la Mer (IFREMER), France (Ezraty et al., 2007) and ice coverage was calculated based on the ARTIST Sea Ice (ASI) algorithm developed at the University of Bremen, Germany (Spreen et al., 2008) at a 12.5×12.5 km resolution.

The environmental sediment parameters were obtained as part of the LTER HAUSGARTEN programme conducted by the AWI. Virtually undisturbed sediment samples were taken in parallel at each station using a multiple corer. Cores were sub-sampled 3–4 times (only once for particulate organic carbon from 2004 to 2008) using plastic syringes (2-cm diameter) modified with the anterior ends cut off and results from the top 1-cm layer used in this study. The majority of pigments (chloroplastic pigment equivalents, CPE) indicate food availability from photosynthetically derived material reaching the seafloor. Phospholipids, representative for the total microbial biomass, were analysed photometrically. Proteins (readily soluble per sediment volume), indicative of living and dead biomass (organisms and detrital matter within the sediments), as well as particulate organic carbon, were also analysed (Jacob et al., 2013; Górska et al., 2014). Table 2 details all MUC deployments.

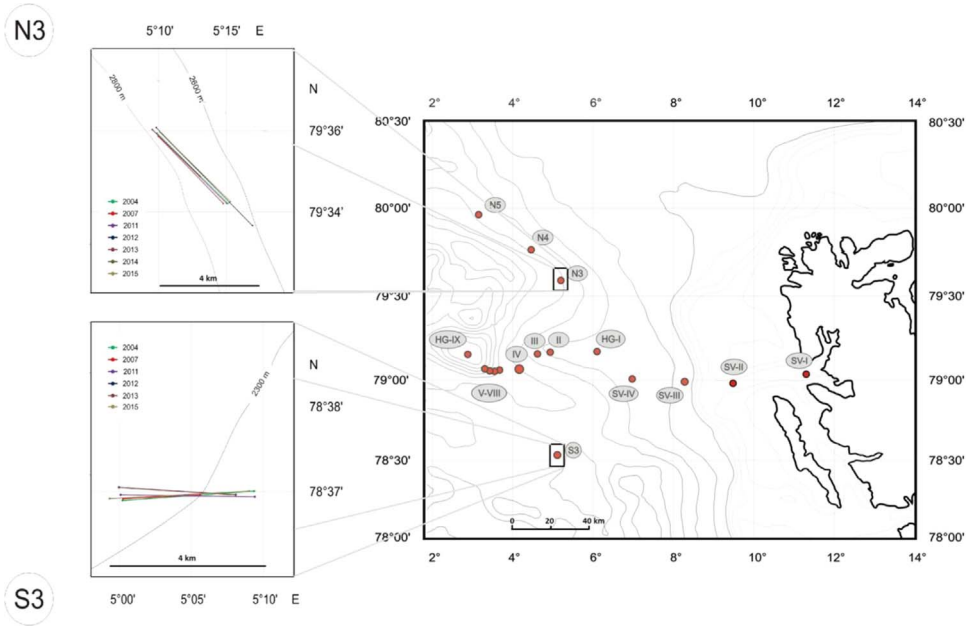

Fig. 1. Map of the LTER observatory HAUSGARTEN and the location of camera transects conducted at stations N3 and S3 from 2004 to 2015.

Table 1
Summary of Ocean Floor Observation System (OFOS) deployments at HAUSGARTEN stations N3 and S3.

Year	Research Vessel	Cruise No.	OFOS Frame (cm)	Make of Still Camera	Lighting & Laser Points
2004	Polarstern	ARK-XX/1	145x225×145	Benthos Inc.	2 high-intensity discharge lights, strobes 3 red LED laser pointers (50 cm distance)
2007	Polarstern	ARK-XXII/1	145x225×145	Benthos model 372-A	2 xenon head lamps (OKTOPUS) 2 flash lights (BENTHOS flash, model 383) 2 green laser pointers (Scholz) (52 cm distance)
2011	Polarstern	ARK-XXVI/2	120x110×120	Canon EOS-1Ds Mark III (modified by Isitec, Germany)	Kongsberg strobe (OE11-242) 4 DeepSea Power & Light LED lights (LED Multi-Sealite) 3 red laser pointers (Oktopus, Germany)
2012	Polarstern	ARK-XXVII/2	140x92×135	Canon EOS-1Ds Mark III (modified by Isitec, Germany)	Kongsberg strobe (OE11-242) 4 DeepSea Power & Light LED lights (LED Multi-Sealite) 3 red laser pointers (Oktopus, Germany)
2013	Maria S. Merian	MSM29	140x92×135	Canon EOS-1Ds Mark III (modified by Isitec, Germany)	Kongsberg strobe (OE11-242) 4 DeepSea Power & Light LED lights (LED Multi-Sealite) 3 red laser pointers (Oktopus, Germany)
2014	Polarstern	ARK-XXVIII/2	140x92×135	Canon EOS-1Ds Mark III (modified by Isitec, Germany)	2 Sea & Sea YS-250PRO (modified by Isitec, Germany) 4 Multi-Sealite LED Lights 3 red laser pointers (Oktopus, Germany) (50 cm distance)
2015	Polarstern	ARK-XXIX/2	140x92×135	Canon EOS 5D Mark III (modified by Isitec, Germany)	2 Sea & Sea YS-250PRO (modified by Isitec, Germany) 4 Multi-Sealite LED Lights 3 red laser pointers (Oktopus, Germany) (50 cm distance)

The abundance of individual habitat features that were recorded alongside the megafaunal abundances for each image included: debris of the sponge *Caulophacus*, stalks of the crinoid *Bathycrinus*, tests of the burrowing sea urchin *Pourtalesia jeffreysi*, shells, dropstones (large stones), pebbles (small stones), burrow entrances and Lebensspuren. "Burrow entrances" were labelled as a separate category to Lebensspuren because of their association with the amphipod *Neohela lamia*. Therefore, Lebensspuren refer purely to animal tracks in this study.

2.5. Data analysis

The megafaunal abundance for each image was extracted from BIIGLE and converted to density (number of ind. m^{-2}). Standard parametric tests (Minitab 17: one-way analysis of variance with Tukey comparisons) were used to compare megafaunal densities, ice coverage and environmental sediment parameters between the years for each station. If non-parametric tests had to be used, due to non-homogenous variance, Kruskal-Wallis followed by pairwise Mann-Whitney *U*-tests were applied using a Bonferroni correction (N3;

Table 2
Summary of gear deployments done at HAUSGARTEN stations N3 and S3. (Lat) latitude, (Lon) longitude, (OFOS) Ocean Floor Observation System, (MUC) multiple corer.

Deployment Number	Sampling Station	Date (dd/mm/yr)	Position Lat (N)	Position Lon (E)	Depth (m)	Gear	No. images taken (no. analysed)
PS62/189-2	S3	10/08/2002	78° 34.97'	5° 04.21'	2344	MUC	
PS62/192-2	N3	11/08/2002	79° 35.02'	5° 15.33'	2668	MUC	
PS64/453-1	S3	30/07/2003	78° 36.50'	5° 04.32'	2343	MUC	
PS66/106-1	S3	08/07/2004	78° 36.97'	5° 00.33'	2363	OFOS (start)	
PS66/106-1	S3	08/07/2004	78° 37.02'	5° 09.90'	2350	OFOS (end)	696 **(66)**
PS66/108-1	S3	08/07/2004	78° 37.50'	5° 03.16'	2349	MUC	
PS66/127-2	N3	11/07/2004	79° 35.93'	5° 09.50'	2791	MUC	
PS66/127-3	N3	11/07/2004	79° 35.99'	5° 10.56'	2784	MUC	
PS66/127-4	N3	11/07/2004	79° 35.90'	5° 09.93'	2788	OFOS (start)	
PS66/127-4	N3	12/07/2004	79° 34.10'	5° 15.18'	2661	OFOS (end)	797 **(80)**
PS68/250-2	N3	21/08/2005	79° 36.23'	5° 10,32'	2784	MUC	
PS68/275-3	S3	25/08/2005	78° 36.59'	5° 04.20'	2339	MUC	
MSM2/803-2	S3	27/08/2006	78° 36.40'	5° 04.12'	2293	MUC	
MSM2/864-1	N3	04/09/2006	79° 36.24'	5° 16.31'	2650	MUC	
PS70/164-1	S3	12/07/2007	78° 36.98'	5° 00.38	2374	OFOS (start)	
PS70/164-1	S3	12/07/2007	78° 37.00'	5° 05.96'	2351	OFOS (end)	520 **(80)**
PS70/174-1	S3	13/07/2007	78° 36.54'	5° 03.82'	2354	MUC	
PS70/197-1	N3	17/07/2007	79° 36.32'	5° 09.23	2804	MUC	
PS70/202-1	N3	17/07/2007	79° 35.82'	5° 10.02'	2800	OFOS (start)	
PS70/202-1	N3	17/07/2007	79° 34.10'	5° 14.83'	2681	OFOS (end)	755 **(80)**
PS72/129-3	S3	10/07/2008	78° 36.48'	5° 03.68'	2343	MUC	
PS72/146-1	N3	14/07/2008	79° 35.75'	5° 10.91'	2781	MUC	
PS74/118-2	N3	16/07/2009	79° 36.24'	5° 10.07'	2787	MUC	
PS74/129-3	S3	18/07/2009	78° 36.48'	5° 04.38'	2340	MUC	
PS76/124-4	S3	04/07/2010	78° 36.37'	5° 03.97'	2341	MUC	
PS76/181-2	N3	15/07/2010	79° 35.69'	5° 13.24	2768	MUC	
PS78/171-1	N3	27/07/2011	79° 35.84'	5° 09.95	2788	OFOS (start)	
PS78/171-1	N3	27/07/2011	79° 34.11'	5° 15.08'	2663	OFOS (end)	304 **(80)**
PS78/171-6	N3	27/07/2011	79° 35.71'	5° 13.26'	2753	MUC	
PS78/182-1	S3	30/07/2011	78° 37.00'	5° 00.19'	2366	OFOS (start)	
PS78/182-1	S3	30/07/2011	78° 36.99'	5° 09.95'	2351	OFOS (end)	365 **(80)**
PS78/182-3	S3	30/07/2011	78° 36.38'	5° 03.92'	2341	MUC	
PS80/176-1	S3	19/07/2012	78° 37.04'	5° 00.07'	2361	OFOS (start)	
PS80/176-1	S3	20/07/2012	78° 37.00'	5° 08.56'	2352	OFOS (end)	672 **(80)**
PS80/176-7	S3	20/07/2012	78° 36.59'	5° 03.96'	2340	MUC	
PS80/188-2	N3	25/07/2012	79° 36.23'	5° 10.23'	2742	MUC	
PS80/193-1	N3	26/07/2012	79° 36.04'	5° 09.88'	2748	OFOS (start)	
PS80/193-1	N3	26/07/2012	79° 33.53'	5° 16.99'	2609	OFOS (end)	778 **(80)**
MSM29/431-3	N3	27/06/2013	79° 35.71'	5° 12.57'	2722	MUC	
MSM29/439-3	S3	01/07/2013	78° 37.20'	5° 01.03'	2318	MUC	
MSM29/440-1	S3	02/07/2013	78° 37.04'	5° 00.08	2316	OFOS (start)	
MSM29/440-1	S3	02/07/2013	78° 37.00'	5° 08.58'	2304	OFOS (end)	573 **(80)**
MSM29/445-1	N3	05/07/2013	79° 35.98'	5° 09.62'	2747	OFOS (start)	
MSM29/445-1	N3	05/07/2013	79° 34.79'	5° 13.13'	2645	OFOS (end)	540 **(80)**
PS85/474-1	N3	26/06/2014	79° 35.92'	5° 10.15'	2721	OFOS (start)	
PS85/474-1	N3	26/06/2014	79° 34.13'	5° 15.29'	2600	OFOS (end)	454 **(80)**
PS93/048-8	S3	24/07/2015	78° 37.02'	5° 09.56'	2351	OFOS (start)	
PS93/048-8	S3	24/07/2015	78° 36.98'	4° 59.39'	2367	OFOS (end)	808 (**80**)
PS93/048-11	S3	25/07/2015	78° 35.98'	5° 04.07'	2342	MUC	
PS93/062-1	N3	03/08/2015	79° 35.92'	5° 10.18'	2787	OFOS (start)	
PS93/062-1	N3	03/08/2015	79° 34.15'	5° 15.36'	2658	OFOS (end)	710 **(80)**
PS93/085-2	N3	11/08/2015	79° 36.25'	5° 10.28'	2783	MUC	

p=0.05/21=0.0024, S3; p=0.05/15=0.0033).

Biota were also grouped in terms of feeding type i.e. predator/scavenger, deposit feeder, suspension feeder and 'not defined' (n.d.) based on information in the literature and advice from specialists (for details see Bergmann et al., 2009; Taylor et al., 2016).

Shannon-Wiener diversity and Pielou's evenness were computed for each image to compare the indices from different years. We also use the additive diversity partition calculations for α (the mean diversity observed within an individual photograph), β (species turnover) and γ (the overall diversity observed at the station as a whole) diversities as described in Taylor et al. (2016):

- α diversity as the mean species number (S) m^{-2} for each year at each station
  i.e. $\alpha = \frac{1}{n} \sum_{image1}^{image\ n} \frac{S}{image\ area}$.
- γ diversity as the total species richness (S_{max}) for each year at each station m^{-2}
  i.e. $\gamma = \frac{1}{n} \sum_{image1}^{image\ n} \frac{S_{max}}{image\ area}$.
- β diversity as the species turnover at a station each year, therefore the difference between the total species richness and the observed species richness
  i.e. $\beta = \gamma - \alpha$.

Routines from multivariate statistics (PRIMER-e 6.1.6, Clarke and Gorley, 2006) were used to determine differences in the community structure based on Bray-Curtis similarity analysis. All density data were square-root transformed to counteract the effect of very abundant taxa. The similarities of different images and transect years were depicted in an ordination biplot (MDS, non-metric multi-dimensional scaling), with each point relating to a single photograph. A one-way ANOSIM routine was used to test for differences between each year at each station. The SIMPER module, based on Bray Curtis similarity, was used

to identify the discriminator species between years. To determine the most important habitat features in explaining the species composition observed the BIOENV module was applied. An ANOSIM and multi-dimensional scaling was also carried out on habitat features recorded for each image (based on Euclidean distance) to see whether any patterns that may have been observable in the biota were due to changes in the environment.

3. Results

The present study is the first to look at temporal variations at multiple stations over a time period longer than a decade. In total, 1026 images were analysed comprising an area of 3669 m^2 (N3=1873 m^2, S3=1796 m^2) with mean areas per image of N3=3.89 ± 0.01 m^2 (± SEM) and S3=3.86 ± 0.02 m^2.

3.1. Taxa recorded

A total of 27 taxa and morphotypes were recorded across all years, with 18 being identified to species level: *Caulophacus arcticus*, *Cladorhiza* cf. *gelida*, cf. *Bathyphellia margaritacea*, *Gersemia fruticosa*, *Byglides groenlandicus*, *Hyalopecten frigidus*, *Ascorhynchus abyssi*, *Neohela lamia*, *Saduria megalura*, *Birsteiniamysis inermis*, *Halirages cainae*, *Kolga hyalina*, *Elpidia heckeri*, *Bathycrinus carpenterii*, *Hymenaster pellucidus*, *Pourtalesia jeffreysi*, *Poliometra prolixa* and *Lycodes frigidus*. The nine organisms that could not be identified to species level included: small round sponge, sponge morphotype 2, purple actinarian, *Candelabrum* sp., *Amphianthus* sp., white long-tentacled actinarian, *Mohnia* spp., *Bythocaris* sp. and isopod. Examples of 20 of these organisms can be found in Fig. 2, with the remaining seven not shown due to a lack of a high quality image being available. The taxonomic grouping "*Mohnia* spp." comprises two gastropod species, *Mohnia mohni* and *Tacita danielsseni*, which are indistinguishable from one another through image analysis. Species accumulation curves (Fig. 3) showed that a sample size of 80 images per transect (S3, 2004=66) was sufficient to capture the taxon inventory as the curves for each transect headed towards a plateau after 15 – 25 images.

3.2. Community structure and megafaunal abundances

There were significant differences at N3 in total megafaunal abundance in different years (K-W, M-W, $p = < 0.0005$, χ^2 =284.22, df =6). Megafaunal abundance was at its lowest in 2004 (12.07 ± 0.39 ind. m^{-2}), whilst the next measured year, 2007 (35.21 ± 0.97 ind. m^{-2}), had the highest abundance, with numbers remaining relatively stable at an elevated level from 2011 onwards. When looking into the broad feeding types of the overall megafaunal abundance of each year, we found significant differences in the numbers of predator/scavengers (ANOVA, $p = < 0.0005$, f =7.71, df =6), suspension feeders (ANOVA, $p = < 0.0005$, f =42.27, df =6) and deposit feeders (K-W, M-W, $p = < 0.0005$, χ^2 =383.27, df =6). For example, deposit feeder numbers increased over 7-fold from 2004 to 2007 (1.97 ± 0.11 to 14.45 ± 0.518 ind. m^{-2} respectively), whilst then declining and levelling off at an elevated level similar to the overall trend (Fig. 4, Fig. 5, Table 3).

Megafaunal abundances at S3 also showed significant variations (K-W, M-W, $p = < 0.0005$, χ^2 =273.42, df =5) in different years with an overall increasing trend over the course of the study. By contrast to N3, lowest numbers were observed in 2007 (11.46 ± 0.27 ind. m^{-2}). After this drop, megafaunal densities increased and peaked in 2015 (22.74 ± 0.61 ind. m^{-2}). There were also significant differences in the numbers of predator/scavengers (K-W, M-W, $p = < 0.0005$, χ^2 =104.43, df =5), suspension feeders (K-W, M-W, $p = < 0.0005$, χ^2 =175.94, df =5) and deposit feeders (K-W, M-W, $p = < 0.0005$, χ^2 =317.83, df =5) across the years. In particular deposit feeders were at their lowest density in 2007 (2.50 ± 0.11 ind. m^{-2}) and attained a 4-fold increase until 2015 (9.70 ± 0.26 ind. m^{-2}) (Fig. 5, Table 4).

Overall, there were significant differences in the community structure at N3 (ANOSIM: Global R =0.550; p=0.001) (Fig. 6). There was a completely separate community in 2004 compared to the other years. From 2007 onwards, there is a continually, gradually changing community as shown by results from ANOSIM comparisons (Table 5). There is also a significant difference in overall community structure between years at S3 (ANOSIM: Global R =0.535; p=0.001, Table 6). S3 does not undergo the same extreme change of community structure between 2004 and 2007 as N3. There is rather a continual change over the studied period (Fig. 6).

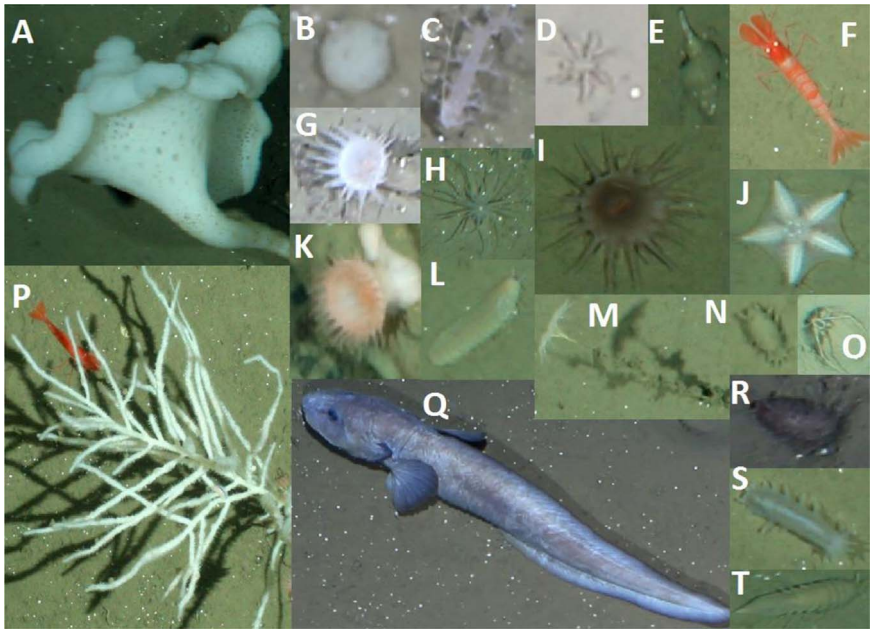

Fig. 2. Examples of taxa/morphotypes from HAUSGARTEN stations N3 and S3: (A) *Caulophacus arcticus*, (B) small round sponge, (C) *Gersemia fruticosa*, (D) *Ascorhynchus abyssi*, (E) *Mohnia* spp., (F) *Bythocaris* sp., (G) cf. *Bathyphellia margaritacea*, (H) white long-tentacled actinarian, (I) purple actinarian, (J) *Hymenaster pellucidus*, (K) *Amphianthus* sp., (L) *Bylgides groenlandicus*, (M) *Bathycrinus carpenterii*, (N) *Elpidia heckeri*, (O) *Neohela lamia*, (P) *Cladorhiza* cf. *gelida*, (Q) *Lycodes frigidus*, (R) *Pourtalesia jeffreysi*, (S) *Kolga hyalina*, (T) *Saduria megalura*.

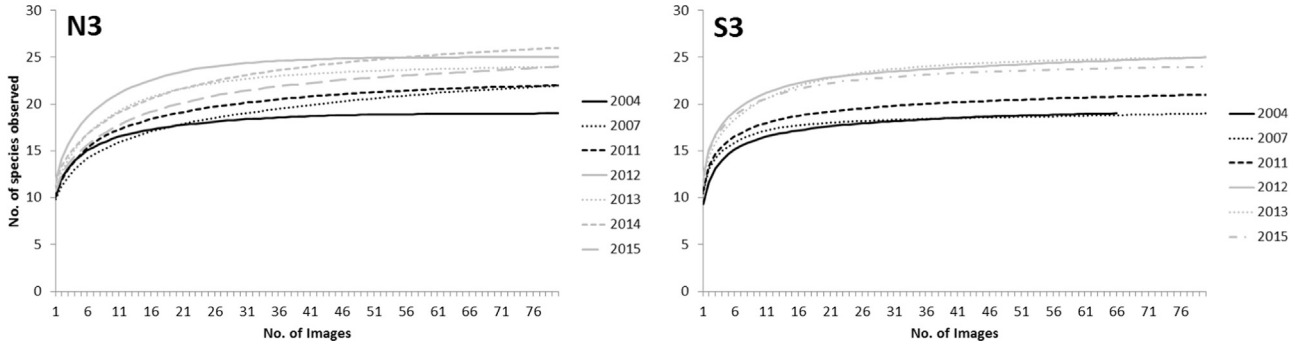

Fig. 3. Species accumulation curves for the 80 (or 66) images from photographic transects taken at HAUSGARTEN stations N3 and S3.

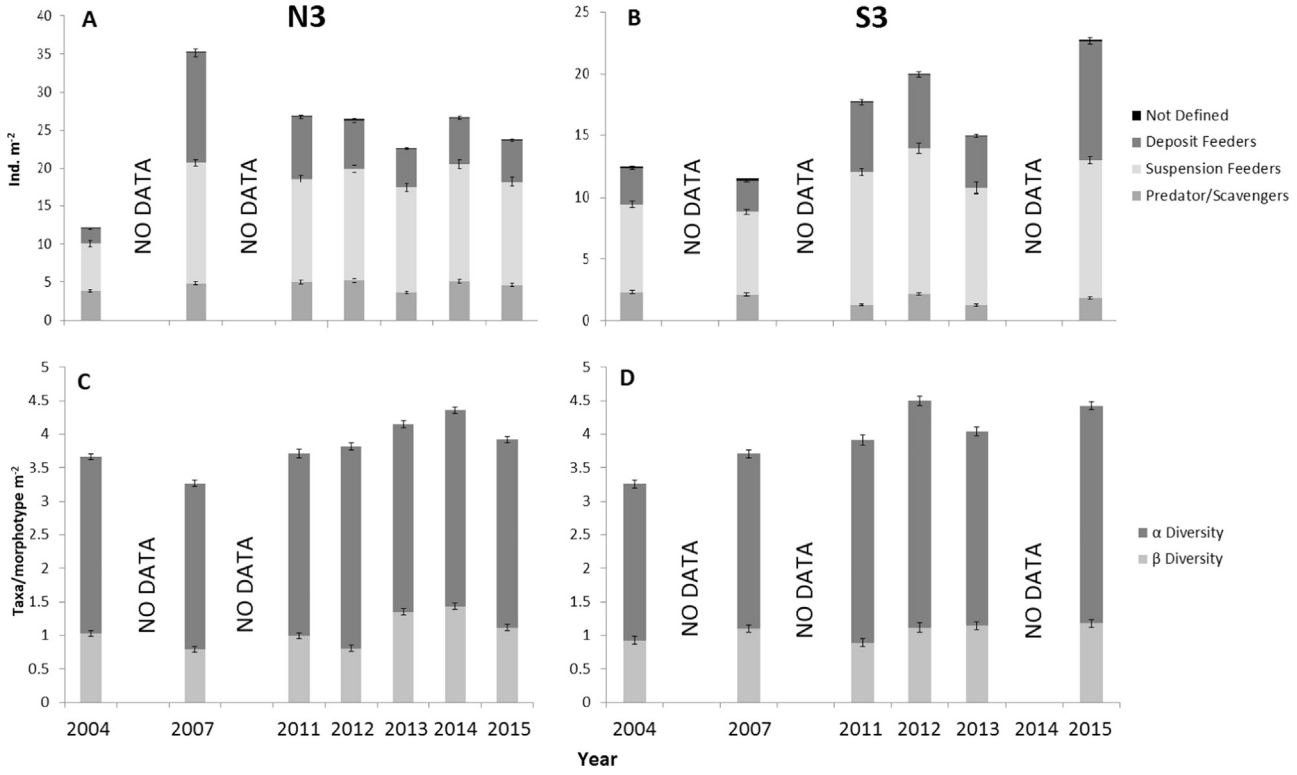

Fig. 4. Mean densities of organisms (ind. m^{-2}) belonging to different feeding types (A & B) and overall gamma (γ) diversity, broken down into alpha (α) and beta (β) components (C & D) recorded from photographic transects taken at HAUSGARTEN stations N3 and S3 for each year.

Two of the largest contributors to the dissimilarity in species composition of different years at N3 are the sea cucumber *Kolga hyalina* and the burrowing amphipod *Neohela lamia* (SIMPER). *Neohela* abundances went from being fairly prevalent in 2004 (2.34 ± 0.16 ind. m^{-2}) to being completely absent from 2007 onwards. By contrast, while *Kolga* was absent in 2004 it peaked in 2007 (5.87 ± 0.22 ind. m^{-2}). From this point, their numbers significantly decreased over the study period (K-W, M-W, $p = < 0.0005$, χ^2 =421.97, df =6) (Fig. 5, Table 3). A smaller holothurian species, *Elpidia heckeri*, also showed significant changes over time, with a 24-fold increase over the years from 2004 (0.09 ± 0.02 ind. m^{-2}) to 2015 (2.19 ± 0.10 ind. m^{-2}) (K-W, M-W, $p = < 0.0005$, χ^2 =261.55, df =6). Another large contributor to the overall dissimilarity was the predatory annelid *Bylgides groenlandicus*. Its density increased approximately 4.5-fold between 2004 (0.39 ± 0.04 ind. m^{-2}) and 2007 (1.79 ± 0.103 ind. m^{-2}) with lower densities in the remaining years, to the point of becoming almost absent (K-W, M-W, $p = < 0.0005$, χ^2 =428.70, df =6). The "purple actinarian" followed a similar trend: it was more abundant in 2004 (1.23 ± 0.08 ind. m^{-2}), decreased in 2007 (0.06 ± 0.02 ind. m^{-2}) and became almost absent thereafter (K-W, M-W, $p = < 0.0005$, χ^2 =450.38, df =6). The sea spider *Ascorhynchus abyssi* also contributed greatly to the observed dissimilarities, showing significant increases in abundances over the whole study period (0.02 ± 0.01 − 1.82 ± 0.10 ind. m^{-2}) (K-W, M-W, $p = < 0.0005$, χ^2 =345.52, df =6). Other taxa/morphotypes producing large contributions to the observed dissimilarities include: the sponges *Caulophacus arcticus*, "small round sponge", "sponge morphotype 2", *Mohnia* spp., "Isopoda" crustacean and the sea lily *Bathycrinus carpenterii*.

At S3, *E. heckeri* and *B. groenlandicus* were the two largest contributors to the overall dissimilarity (SIMPER). *Elpidia* abundances significantly increased 5-fold over the study period with highest numbers in 2015 (3.74 ± 0.14 ind. m^{-2}), and the second largest peak in 2011 (0.78 ± 0.07 ind. m^{-2}) (K-W, M-W, $p = < 0.0005$, χ^2 =253.78, df =5). *Bylgides* abundances in 2004 (0.40 ± 0.04 ind. m^{-2}) and 2007 (1.15 ± 0.07 ind. m^{-2}) were significantly higher than in other years, with 2007 being particularly high (K-W, M-W, $p = < 0.0005$, χ^2 =297.83, df =5).

The anemone *Amphianthus* sp. (K-W, M-W, $p = < 0.0005$, χ^2 =200.02, df =5) and "Isopoda" (K-W, M-W, $p = < 0.0005$, χ^2 =242.52, df =5) also contributed to the overall dissimilarity, with large increases over the course of the study. *Amphianthus* sp. only emerged from 2011 onwards. Other contributors included "small round sponge", "sponge

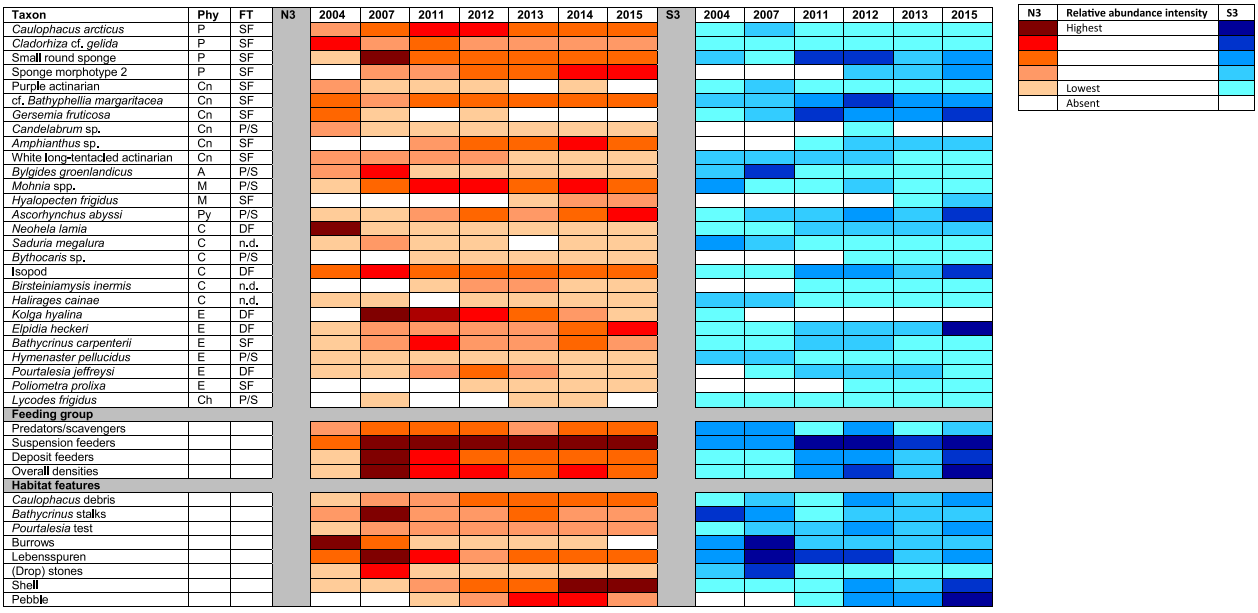

Fig. 5. Heatmap showing the relative abundance of each taxa/morphotype, trophic feeding type (FT) and environmental variable at HAUSGARTEN stations N3 and S3. Different colour shades indicate a significant difference in abundance between subsequent years (Bonferroni: N3; p=0.05/21=0.0024, S3; p=0.05/15=0.0033); (Phy) Phylum: (P) Porifera, (Cn) Cnidaria, (A) Annelida, (M) Mollusca, (Py) Pycnogonida, (C) Crustacea, (E) Echinodermata, (Ch) Chordata (see Tables 3 and 4 for abundance data).

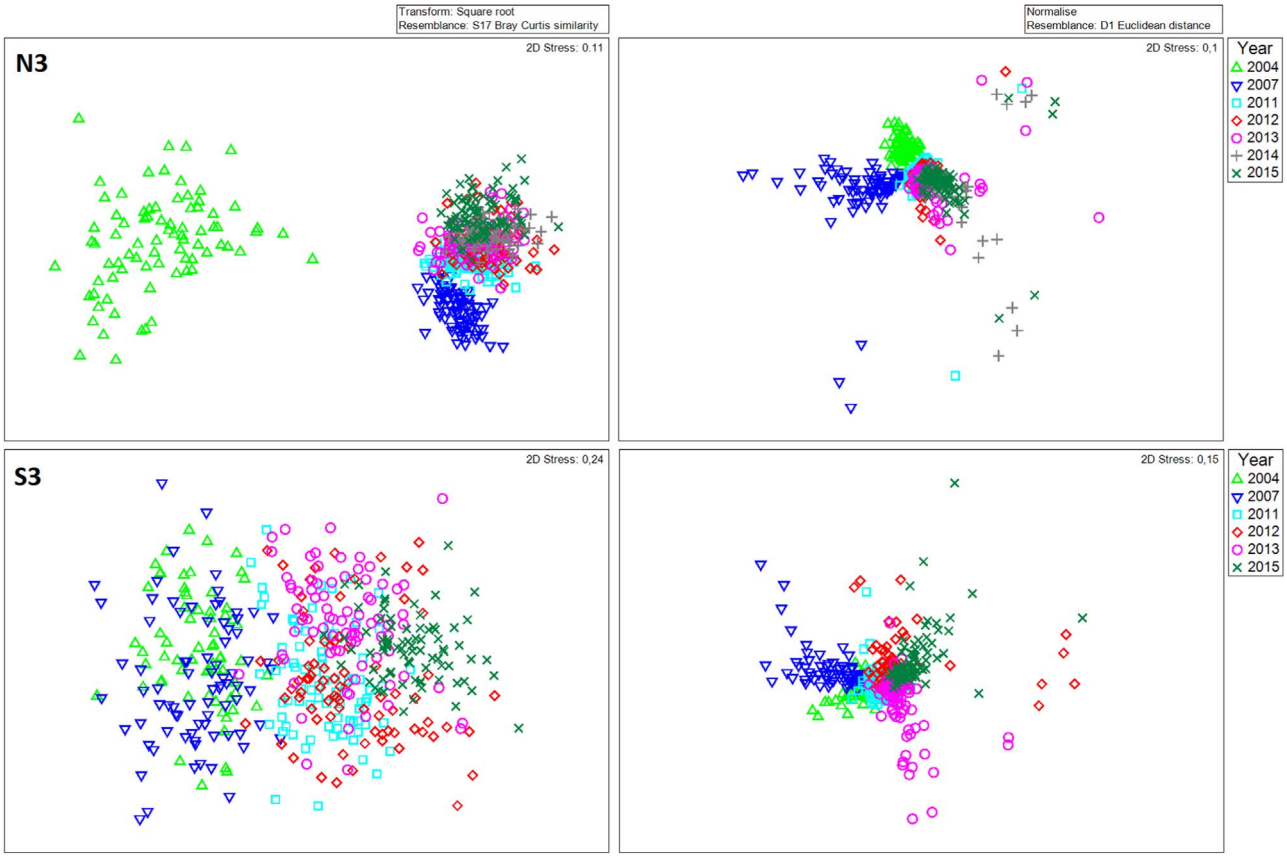

Fig. 6. MDS plots depicting community (left) and benthic (right) habitat feature composition from photographic transects taken at HAUSGARTEN stations N3 (above) and S3 (below). Each point relates to one image.

morphotype 2", the soft coral *Gersemia fruticosa*, white long-tentacled actinarians and *Mohnia* spp.

There were significant temporal differences in Shannon-Wiener diversity (K-W, M-W, $p = < 0.0005$, χ^2 =194.97, df =6) and Pielou's evenness (ANOVA, $p = < 0.0005$, f =41.84, df =6) at N3. Both peaked in 2004 (H' =2.00 ± 0.02; J' =0.87 ± 0.01), before a decrease in 2007 (H' =1.781 ± 0.01; J' =0.78 ± 0.01) with a gradual increase from that point onwards. Significant differences were also observed between years in α diversity (ANOVA, p= < 0.0005, f =12.12, df =6), β diversity (K-W, M-W, p= < 0.0005, χ^2 =29.96, df =6) and γ diversity (ANOVA, p= < 0.0005, f =310.63, df =6). Overall, there was an increase in species richness at N3. Fig. 4 shows that 2012 and 2013 had a greater

Table 3
Mean densities (ind. m^{-2}) of megafaunal taxa/morphotypes, habitat features and diversity indices recorded from photographic transects conducted at HAUSGARTEN station N3 (* indicates taxa/morphotypes indicated by SIMPER that cause the greatest dissimilarities).

Taxon – N3	FT	2004 Mean	± SE	2007 Mean	± SE	2011 Mean	± SE	2012 Mean	± SE	2013 Mean	± SE	2014 Mean	± SE	2015 Mean	± SE	Test Used	*p*	*f* or χ2
Porifera																		
Caulophacus arcticus *	SF	0.023	0.013	0.216	0.037	0.509	0.117	0.473	0.097	0.251	0.047	0.330	0.062	0.316	0.057	K-W, M-W	< 0.0005	43.55
Cladorhiza cf. *gelida*	SF	0.260	0.038	0.009	0.005	0.144	0.024	0.065	0.013	0.038	0.011	0.066	0.014	0.049	0.014			
Small round sponge *	SF	1.405	0.147	11.598	0.414	6.807	0.349	7.547	0.258	7.104	0.245	6.625	0.209	5.505	0.233	K-W, M-W	< 0.0005	305.00
Sponge morphotype 2	SF			0.028	0.028	0.237	0.072	1.615	0.251	1.650	0.213	2.695	0.373	2.676	0.359	K-W. M-W	< 0.0005	296.30
Cnidaria																		
Purple actinarian *	SF	1.226	0.075	0.055	0.017	0.006	0.004	0.012	0.006			0.004	0.004			K-W, M-W	< 0.0005	450.38
cf. *Bathyphellia margaritacea*	SF	1.517	0.153	1.159	0.073	1.753	0.089	1.583	0.080	1.670	0.099	1.750	0.086	1.587	0.086			
Gersemia fruticosa	SF	0.685	0.068	0.006	0.004			0.013	0.006									
Candelabrum sp.	P/S			0.013	0.008	0.004	0.004	0.022	0.009	0.010	0.005	0.009	0.005	0.010	0.006			
Amphianthus sp.	SF							0.217	0.031	0.186	0.033	0.278	0.042	0.164	0.032			
White long-tentacled actinarian	SF	0.095	0.022	0.091	0.017	0.117	0.023	0.070	0.021	0.034	0.011	0.016	0.009	0.023	0.010			
Annelida																		
Bylgides groenlandicus *	P/S	0.390	0.036	1.794	0.103	0.031	0.011	0.042	0.012	0.020	0.008	0.010	0.007	0.003	0.003	K-W, M-W	< 0.0005	428.70
Mollusca																		
Mohnia spp. *	P/S	0.952	0.070	2.764	0.153	3.979	0.196	3.711	0.237	2.805	0.144	3.826	0.204	2.730	0.185	K-W, M-W	< 0.0005	214.98
Hyalopecten frigidus	SF									0.082	0.021	0.227	0.032	0.202	0.026			
Pycnogonida																		
Ascorhynchus abyssi *	P/S	0.016	0.007	0.158	0.024	0.966	0.084	1.334	0.089	0.740	0.051	1.191	0.064	1.820	0.096	K-W, M-W	< 0.0005	345.52
Crustacea																		
Neohela lamia *	DF	2.338	0.164	0.003	0.003	0.010	0.007	0.016	0.007	0.006	0.006	0.003	0.003	0.007	0.007	K-W, M-W	< 0.0005	497.74
Saduria megalura	n.d.	0.017	0.007	0.034	0.011	0.011	0.006	0.026	0.009			0.004	0.004	0.003	0.003			
Bythocaris sp.	P/S					0.034	0.011	0.025	0.009	0.021	0.012	0.028	0.011	0.030	0.012			
Isopoda *	DF	1.878	0.019	7.456	0.523	2.366	0.150	2.212	0.155	1.656	0.089	2.805	0.122	2.078	0.106	K-W, M-W	< 0.0005	132.48
Birsteiniamysis inermis	n.d.					0.022	0.009	0.071	0.014	0.048	0.011	0.015	0.007	0.023	0.008			
Halirages cainae	n.d.	0.065	0.015	0.043	0.011			0.035	0.010	0.029	0.009	0.048	0.017	0.026	0.009			
Echinodermata																		
Kolga hyalina *	DF			5.866	0.220	4.562	0.142	2.809	0.165	2.379	0.085	1.783	0.094	1.156	0.100	K-W, M-W	< 0.0005	421.97
Elpidia heckeri *	DF	0.090	0.018	1.125	0.083	1.183	0.062	1.162	0.069	1.037	0.064	1.448	0.081	2.188	0.097	K-W, M-W	< 0.0005	261.55
Bathycrinus carpenterii *	SF	0.978	0.100	2.756	0.096	3.926	0.116	3.108	0.117	2.762	0.130	3.435	0.143	3.081	0.130	ANOVA	< 0.0005	59.55
Hymenaster pellucidus	P/S	0.046	0.013	0.025	0.008	0.012	0.006	0.031	0.009	0.013	0.007	0.029	0.009	0.017	0.007			
Pourtalesia jeffreysi	DF	0.006	0.004	0.003	0.003	0.057	0.016	0.212	0.025	0.090	0.020	0.025	0.009	0.009	0.009			
Poliometra prolixa	SF							0.015	0.008	0.021	0.009	0.043	0.014	0.026	0.013			
Chordata																		
Lycodes frigidus	P/S			0.010	0.006					0.023	0.010	0.009	0.005					
Feeding Type																		
Predators/ scavengers		3.843	0.196	4.800	0.212	5.012	0.249	5.183	0.273	3.617	0.167	5.081	0.216	4.590	0.236	ANOVA	< 0.0005	7.71
Suspension feeders		6.189	0.378	15.919	0.458	13.593	0.490	14.719	0.483	13.797	0.499	15.469	0.595	13.629	0.595	ANOVA	< 0.0005	42.27
Deposit feeders		1.974	0.105	14.451	0.518	8.167	0.204	6.395	0.254	5.162	0.146	6.061	0.184	5.431	0.171	K-W, M-W	< 0.0005	383.27
Not defined		0.065	0.015	0.043	0.011	0.056	0.015	0.131	0.018	0.099	0.017	0.092	0.021	0.079	0.016	ANOVA	0.003	3.30
Overall densities		12.072	0.389	35.214	0.967	26.828	0.795	26.428	0.776	22.674	0.652	26.703	0.812	23.729	0.835	K-W, M-W	< 0.0005	284.22
Diversity indices																		
Shannon-Wiener *H*		2.000	0.019	1.781	0.011	1.958	0.013	2.045	0.013	1.983	0.018	2.081	0.012	2.079	0.014	K-W, M-W	< 0.0005	194.97

(continued on next page)

Table 3 *(continued)*

Taxon – N3	FT	2004 Mean	± SE	2007 Mean	± SE	2011 Mean	± SE	2012 Mean	± SE	2013 Mean	± SE	2014 Mean	± SE	2015 Mean	± SE	Test Used	*p*	*f* or χ2
Pielou's evenness *J*		0.869	0.006	0.784	0.005	0.848	0.004	0.832	0.005	0.839	0.005	0.859	0.005	0.881	0.005	ANOVA	< 0.0005	41.84
α diversity		2.630	0.044	2.474	0.043	2.713	0.063	3.006	0.051	2.798	0.056	2.923	0.049	2.802	0.050	ANOVA	< 0.0005	12.12
γ diversity		3.658	0.027	3.266	0.026	3.709	0.044	3.814	0.031	4.150	0.030	4.355	0.035	3.918	0.027	K-W, M-W	< 0.0005	310.63
β diversity		1.029	0.041	0.792	0.036	0.995	0.044	0.807	0.049	1.351	0.049	1.432	0.049	1.116	0.046	ANOVA	< 0.0005	29.96
Habitat features																		
Caulophacus debris		0.058	0.021	0.907	0.128	0.962	0.161	1.851	0.417	1.511	0.195	1.874	0.258	1.872	0.320	K-W, M-W	< 0.0005	172.52
Bathycrinus stalks		1.832	0.107	3.973	0.152	1.751	0.099	2.000	0.093	2.189	0.093	1.692	0.077	1.641	0.085	K-W, M-W	< 0.0005	159.77
Pourtalesia test		0.003	0.003	0.554	0.221			0.662	0.234	0.289	0.057	0.651	0.170	0.488	0.107	ANOVA	0.025	2.43
Burrows		22.000	0.704	7.301	0.690	0.121	0.024	0.497	0.096	0.009	0.005	0.010	0.006			K-W, M-W	< 0.0005	461.06
Lebensspuren		13.033	0.230	26.565	0.371	15.524	0.260	11.798	0.115	13.613	0.138	13.232	0.150	13.618	0.119	K-W, M-W	< 0.0005	316.02
(Drop) stones		0.365	0.051	3.130	0.336	0.112	0.022	0.134	0.022	0.140	0.023	0.135	0.022	0.154	0.028	K-W, M-W	< 0.0005	207.11
Shell		0.007	0.005	0.069	0.013	0.881	0.077	1.843	0.126	1.969	0.114	5.843	0.286	6.064	0.298	ANOVA	0.134	1.64
Pebble						15.703	1.813	39.684	2.663	84.499	7.696	85.415	4.316	63.993	4.169	K-W, M-W	< 0.0005	482.12

Table 4
Mean densities (ind. m^{-2}) of megafaunal taxa/morphotypes, habitat features and diversity indices recorded from photographic transects conducted at HAUSGARTEN station S3 (* indicates taxa/morphotypes indicated by SIMPER that cause the greatest dissimilarities).

Taxon – S3	FT	2004 Mean	± SE	2007 Mean	± SE	2011 Mean	± SE	2012 Mean	± SE	2013 Mean	± SE	2015 Mean	± SE	Test Used	*p*	*f* or χ2
Porifera																
Caulophacus arcticus	SF	0.012	0.010	0.104	0.036	0.020	0.008	0.063	0.021	0.034	0.015	0.032	0.011			
Cladorhiza cf. *gelida*	SF	0.094	0.021	0.050	0.017	0.058	0.015	0.122	0.026	0.089	0.025	0.067	0.017			
Small round sponge *	SF	4.457	0.169	3.437	0.139	6.181	0.210	6.113	0.216	4.817	0.129	5.212	0.143	K-W, M-W	< 0.0005	140.21
Sponge morphotype 2 *	SF							0.726	0.165	0.326	0.066	1.249	0.300	K-W, M-W	< 0.0005	161.28
Cnidaria																
Purple actinarian	SF	0.223	0.034	0.328	0.034	0.245	0.034	0.209	0.026	0.223	0.030	0.212	0.026			
cf. *Bathyphellia margaritacea*	SF	1.295	0.108	1.502	0.077	1.873	0.104	2.089	0.096	1.791	0.079	1.784	0.094			
Gersemia fruticosa *	SF	0.143	0.033	0.308	0.035	0.733	0.061	0.516	0.062	0.546	0.058	0.795	0.064	K-W, M-W	< 0.0005	107.81
Candelabrum sp.	P/S							0.004	0.004							
Amphianthus sp. *	SF					0.405	0.089	0.732	0.167	0.972	0.121	0.935	0.103	K-W, M-W	< 0.0005	200.02
White long-tentacled actinarian *	SF	0.423	0.057	0.499	0.063	0.439	0.056	0.406	0.049	0.075	0.017	0.095	0.023	K-W, M-W	< 0.0005	91.43
Annelida																
Bylgides groenlandicus *	P/S	0.400	0.040	1.148	0.073	0.072	0.020	0.040	0.011	0.025	0.010	0.033	0.011	K-W, M-W	< 0.0005	297.83
Mollusca																
Mohnia spp. *	P/S	1.651	0.104	0.542	0.039	0.545	0.045	1.136	0.079	0.622	0.047	0.703	0.048	K-W, M-W	< 0.0005	126.81
Hyalopecten frigidus	SF									0.031	0.015	0.095	0.017			

(continued on next page)

Table 4 *(continued)*

Taxon – S3	FT	2004 Mean	± SE	2007 Mean	± SE	2011 Mean	± SE	2012 Mean	± SE	2013 Mean	± SE	2015 Mean	± SE	Test Used	*p*	*f* or χ2
Pycnogonida																
Ascorhynchus abyssi *	P/S	0.036	0.012	0.283	0.037	0.315	0.042	0.550	0.048	0.234	0.030	0.665	0.041	K-W, M-W	< 0.0005	151.05
Crustacea																
Neohela lamia	DF	0.078	0.017	0.058	0.016	0.295	0.040	0.333	0.038	0.291	0.027	0.352	0.031			
Saduria megalura	n.d.	0.100	0.020	0.044	0.011	0.013	0.006	0.017	0.008	0.010	0.005	0.010	0.005			
Bythocaris sp.	P/S							0.042	0.016	0.047	0.020	0.054	0.013			
Isopoda *	DF	2.530	0.113	2.110	0.104	4.723	0.193	5.106	0.220	3.276	0.119	5.804	0.188	K-W, M-W	< 0.0005	242.52
Birsteiniamysis inermis	n.d.					0.040	0.011	0.063	0.016	0.028	0.010	0.051	0.012			
Halirages cainae	n.d.	0.096	0.023	0.085	0.015	0.048	0.013	0.053	0.013			0.016	0.007			
Echinodermata																
Kolga hyalina	DF	0.011	0.006													
Elpidia heckeri *	DF	0.312	0.044	0.240	0.027	0.775	0.067	0.647	0.051	0.619	0.044	3.739	0.139	K-W, M-W	< 0.0005	253.78
Bathycrinus carpenterii	SF	0.552	0.050	0.546	0.045	0.810	0.056	0.799	0.064	0.623	0.050	0.673	0.049			
Hymenaster pellucidus	P/S	0.026	0.009	0.022	0.009	0.003	0.003	0.003	0.003	0.010	0.006					
Pourtalesia jeffreysi	DF			0.153	0.021	0.203	0.026	0.256	0.030	0.249	0.029	0.153	0.019			
Poliometra prolixa	SF							0.035	0.011	0.025	0.011	0.012	0.006			
Chordata																
Lycodes frigidus	P/S	0.004	0.004	0.004	0.004	0.006	0.004	0.014	0.007	0.003	0.003	0.003	0.003			
Feeding type																
Predators/ scavengers		2.295	0.117	2.100	0.110	1.251	0.070	2.141	0.107	1.241	0.071	1.819	0.069	K-W, M-W	< 0.0005	104.43
Suspension feeders		7.199	0.250	6.773	0.195	10.764	0.306	11.809	0.408	9.552	0.295	11.161	0.458	K-W, M-W	< 0.0005	175.94
Deposit feeders		2.854	0.122	2.503	0.108	5.700	0.208	6.010	0.233	4.145	0.127	9.696	0.262	K-W, M-W	< 0.0005	317.83
Not defined		0.096	0.023	0.085	0.015	0.088	0.018	0.116	0.021	0.077	0.018	0.067	0.014	ANOVA	0.517	0.85
Overall densities		12.444	0.318	11.462	0.273	17.803	0.446	20.075	0.531	15.014	0.347	22.744	0.610	K-W, M-W	< 0.0005	273.42
Diversity indices																
Shannon-Wiener *H*		2.084	0.025	2.234	0.020	2.204	0.021	2.315	0.020	2.286	0.021	2.359	0.016	ANOVA	< 0.0005	20.96
Pielou's evenness *J*		0.942	0.002	0.956	0.002	0.933	0.002	0.936	0.002	0.944	0.002	0.938	0.002	ANOVA	< 0.0005	21.57
α diversity		2.332	0.061	2.605	0.059	3.023	0.078	3.380	0.074	2.895	0.068	3.243	0.061	ANOVA	< 0.0005	31.90
γ diversity		3.256	0.031	3.710	1.105	3.914	0.057	4.495	0.041	4.042	0.032	4.419	0.048	K-W, M-W	< 0.0005	265.03
β diversity		0.924	0.059	1.104	0.052	0.891	0.061	1.115	0.070	1.146	0.059	1.177	0.056	ANOVA	0.001	4.02
Habitat features																
Caulophacus debris		0.157	0.030	0.342	0.048	0.137	0.029	0.498	0.064	0.326	0.045	0.542	0.066	K-W, M-W	< 0.0005	56.92
Bathycrinus stalks		1.541	0.104	1.145	0.070	0.438	0.046	0.657	0.056	0.567	0.046	0.666	0.051	K-W, M-W	< 0.0005	128.86
Pourtalesia tests		0.071	0.019	0.178	0.034	0.169	0.035			0.221	0.032	0.354	0.031	K-W, M-W	< 0.0005	70.97
Burrows		2.900	0.164	5.117	0.233	1.774	0.111	1.417	0.093	1.559	0.092	1.454	0.098	K-W, M-W	< 0.0005	202.26
Lebensspuren		13.697	0.267	17.701	0.435	15.599	0.352	15.424	0.301	12.003	0.128	13.408	0.259	K-W, M-W	< 0.0005	161.26
(Drop) stones		0.389	0.041	1.418	0.080	0.109	0.023	0.177	0.032	0.103	0.020	0.221	0.042	K-W, M-W	< 0.0005	222.89
Shells		0.008	0.006	0.012	0.006	0.065	0.017	0.689	0.058	0.369	0.040	1.389	0.088	ANOVA	0.011	3.00
Pebbles						1.141	0.132	6.447	0.546	6.121	0.285	17.379	0.728	K-W, M-W	< 0.0005	325.99
Algal debris										0.313	0.043	0.003	0.003	K-W, M-W	< 0.0005	420.27

Table 5
ANOSIM results of the community structure and habitat feature composition taken from photographic transects at HAUSGARTEN station N3.

Years compared	ANOSIM community structure (*R*)	ANOSIM habitat feature composition (*R*)
2004 v 2007	0.986	0.739
2004 v 2011	0.989	0.862
2004 v 2012	0.993	0.834
2004 v 2013	0.989	0.770
2004 v 2014	0.993	0.810
2004 v 2015	0.992	0.840
2007 v 2011	0.734	0.583
2007 v 2012	0.824	0.654
2007 v 2013	0.841	0.601
2007 v 2014	0.939	0.695
2007 v 2015	0.949	0.685
2011 v 2012	0.249	0.252
2011 v 2013	0.342	0.274
2011 v 2014	0.457	0.536
2011 v 2015	0.581	0.511
2012 v 2013	0.084	0.075
2012 v 2014	0.186	0.304
2012 v 2015	0.308	0.303
2013 v 2014	0.157	0.188
2013 v 2015	0.262	0.238
2014 v 2015	0.126	0.036

Table 6
ANOSIM results of the community structure and habitat feature composition taken from photographic transects at HAUSGARTEN station S3.

Years compared	ANOSIM community structure (*R*)	ANOSIM habitat feature composition (*R*)
2004 v 2007	0.355	0.306
2004 v 2011	0.651	0.370
2004 v 2012	0.624	0.323
2004 v 2013	0.748	0.354
2004 v 2015	0.957	0.672
2007 v 2011	0.626	0.492
2007 v 2012	0.656	0.454
2007 v 2013	0.707	0.542
2007 v 2015	0.913	0.717
2011 v 2012	0.107	0.199
2011 v 2013	0.229	0.304
2011 v 2015	0.505	0.624
2012 v 2013	0.196	0.162
2012 v 2015	0.380	0.221
2013 v 2015	0.451	0.345

contribution to overall species richness (γ) due to species turnover (β), whilst the other years showed similar contributions of α and β diversity to overall species richness.

There were significant temporal differences in Shannon-Wiener diversity (ANOVA, p= < 0.0005, f =20.96, df =5) and Pielou's evenness (ANOVA, p= < 0.0005, f =21.57, df =5) at S3, with increasing diversity and evenness fluctuating over time. Significant differences were also observed between years in α diversity (ANOVA, p= < 0.0005, f =31.90, df =5), β diversity (ANOVA, p= < 0.0005, f =4.02, df =5) and γ diversity (K-W, M-W, p 0 < 0.0005, χ^2 =265.03, df =5). As with N3, there was an overall increase in species richness with consistent levels of α and β diversity to overall species richness (Fig. 4).

3.3. Habitat feature composition and abundances

There were significant differences overall in the similarity of the habitat feature composition at N3 between years (ANOSIM: Global R =0.485, p=0.001). The habitat features from 2004 and 2007 were distinct from those recorded between 2011 and 2015 (Table 5). The BIOENV module showed that the single most important habitat feature in describing species composition was burrow entrances (correlation coefficient 0.732). The highest burrow counts were observed in 2004 (22.00 ± 0.70 ind. m^{-2}), followed by a 3-fold decrease in 2007 (7.30 ± 0.69 ind. m^{-2}) and a continual decrease thereafter (K-W, M-W, p= < 0.0005, χ^2 =461.06, df =6). The second most important habitat feature to explain species composition was (drop-)stone abundance. These were significantly more prevalent in 2007 (3.13 ± 0.34 ind. m^{-2}) with a 10-fold increase from 2004, coinciding with the largest overall mega-faunal abundances at N3 (K-W, M-W, p= < 0.0005, χ^2 =207.11, df =6).

There was also a significant difference in the composition of habitat features between the years at S3 (ANOSIM: Global R =0.390; p=0.001). The combination of burrows, (drop-)stones, *Bathycrinus* stalks and "pebble" were most important in describing species composition, albeit with a weak/moderate correlation value of 0.378 (BIOENV). Univariate statistics corroborated these results: both burrow (K-W, M-W, p= < 0.0005, χ^2 =202.26, df =5) and (drop)-stone (K-W, M-W, p= < 0.0005, χ^2 =222.89, df =5) densities were significantly highest in 2007 (5.12 ± 0.23; 1.42 ± 0.08 ind. m^{-2} respectively) followed by 2004 (2.90 ± 0.16; 0.39 ± 0.04 ind. m^{-2} respectively) and were low thereafter (Fig. 5). Pebble numbers significantly increased over the course of the study, with a 3-fold increase from 2013 (6.12 ± 0.285 ind. m^{-2}) to 2015 (17.38 ± 0.73 ind. m^{-2}) (K-W, M-W, p= < 0.0005, χ^2 =325.99, df =5) (Fig. 5).

3.3.1. Environmental sediment parameters

There were significant differences at N3 in the biogeochemical sediment parameters phospholipids (ANOVA, p=0.027, f =2.51, df =11) and CPE (ANOVA, p < 0.0005, f =18.00, df =11) (Fig. 7). Of particular note is the significant increase observed in CPE in 2007, after which concentrations remain at an elevated level.

At S3, there were also significant differences in phospholipids (ANOVA, p=0.002, f =4.12, df =11) and CPE (ANOVA, p < 0.0005, f =30.02, df =12). As with N3, there were increased levels of CPE from 2007 onwards (Fig. 7). Concentrations of CPE were similar to those from N3, but phospholipids were generally lower at S3 (Fig. 7). However, at both stations there was no significant variation in readily soluble protein or particulate organic carbon.

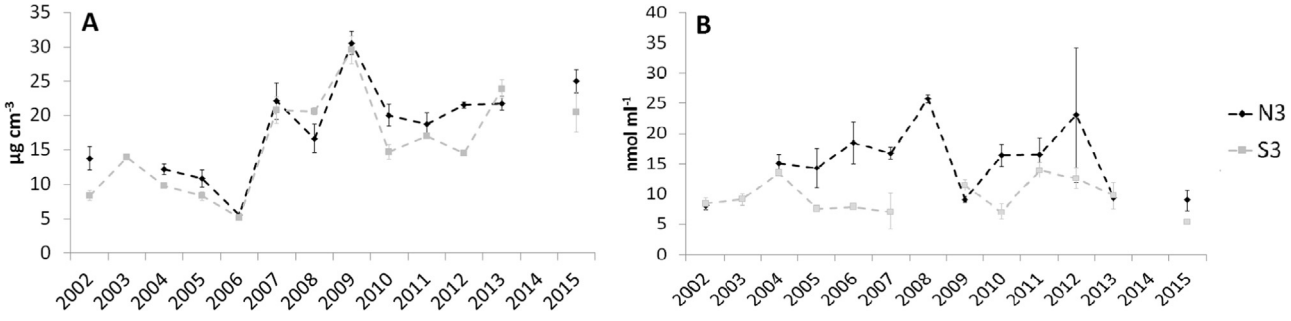

Fig. 7. Environmental sediment parameters measured at HAUSGARTEN stations N3 (black diamonds) and S3 (grey squares) from 2004 to 2015: Mean concentrations in (A) chloroplastic pigment equivalents (CPE) and (B) phospholipids. Line breaks indicate a lack of data available. Error bars indicate the standard error of the mean.

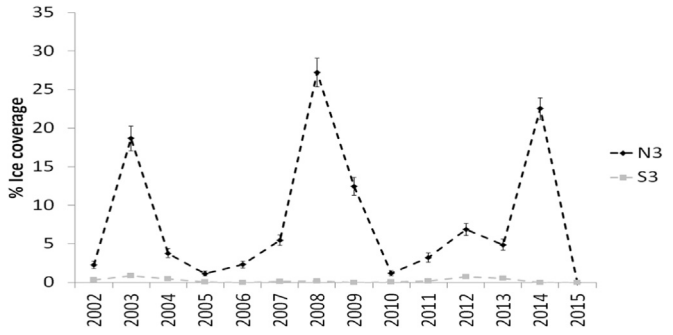

Fig. 8. A plot of the yearly mean average of sea-ice coverage at HAUSGARTEN stations N3 and S3 from 2004 to 2015.

3.4. Sea-ice data

Between January 2002 and August 2015 there were significant differences in ice coverage at N3 (K-W, M-W, $p = < 0.0005$, $\chi^2 = 792.02$, df =13) with peaks during the summers of 2003 and 2014, and a maximum in 2008 (88.23 ± 2.04% coverage) (Fig. 8). At S3, there were also significant differences in ice coverage (K-W, M-W, $p = < 0.0005$, $\chi^2 = 49.39$, df =13) although this station was predominantly ice free. This is due to small peaks in 2003 (10.93 ± 3.189% coverage), 2012 (8.13 ± 2.61% coverage) and 2013 (5.97 ± 2.00% coverage) (Fig. 8).

4. Discussion

Our study is one of the first to investigate differences in deep-sea epibenthic megafauna over a longer term (> 10 years) temporal scale in the Arctic. It is also the first study to assess temporal changes in species diversity and turnover of megafauna in the HAUSGARTEN region. There were high levels of taxonomic overlap between the years studied. Therefore, it is the proportion of each of the species present, rather than differences in the species inventory, that caused the overall temporal variability. This concurs with results from HAUSGARTEN stations IV (Bergmann et al., 2011) and I (Meyer et al., 2013).

Over the course of the study the OFOS setup was subject to constant upgrades to improve image quality, illumination and usability. Changes in the configuration are not ideal for a time-series study, but the continual development of technology improves the data and increases scientific power. Whilst it cannot be excluded that it may have biased our results, the authors believe that everything that could be done to minimise the impact (e.g. exclusion of inappropriately lit or unfocused images) was implemented and that the integrity of the study remains intact. All images used were of sufficient quality to identify organisms greater than 1.5 cm. We also justify our reasoning by the largest abundances of epibenthic megafauna being observed in 2007 at N3 a year with the lowest quality of images, showing that the OFOS set up was still of sufficient quality for the identification of all observed taxa.

Schoening et al. (2012) and Durden et al. (2016) pointed out the potential for high individual error and inter-observer variability when annotating images or video clips, especially on those taxa/morphotypes that blend into their environment. During our study, each image was annotated by a single expert twice to alleviate these issues, with additional quality control from other experts on a subset of images.

Another potential limitation of our study is that of the influence of spatial variation of biota and habitat features. Taylor et al. (2016) specifically studied spatial variation in community structure within both N3 and S3. Due to obvious technical and ship time constraints all data in Taylor et al. (2016) and this manuscript are based on images taken from a single transect at each station, each year. Transects in Taylor et al. (2016) were divided into three separate sections with no overlap, essentially producing three transects, each containing 40 images, which were treated as replicates when performing statistical tests. This could be considered pseudo-replication. However, because of the long time that it would have taken to repeatedly lower the OFOS to the deep seafloor for proper replication at one station and constraints in ship time we considered this the most feasible approach to study spatial variability. Other studies also adopted similar approaches (e.g. Teixidó et al., 2004, 2007; MacDonald et al., 2010). There were no significant variations in community structure between any of the sections at stations N3 or S3 over the course of a 4 km transect in Taylor et al. (2016), and, as is visible in Fig. 1, maximum distance between transect replicates of consecutive years is only approximately 300 m. Therefore, whilst it cannot be ruled out that spatial variation is a potential influencing factor, the authors favour the explanation that most of the observed variation is dominated by temporal influences rather than spatial heterogeneity.

4.1. Variations in community structure, density and diversity indices

Our results show that there are temporal dissimilarities in the benthic megafaunal communities at both N3 and S3, with completely separate communities being observed in 2004 than in 2015. Previously, Billett et al. (2010) suggested that magnitude changes in densities of invertebrate megafauna could be observed over periods as short as six months at the Porcupine Abyssal Plain (PAP). The PAP findings (Billett et al., 2010) were corroborated by results in meiofauna (Gooday et al., 2009; Kalogeropoulou et al., 2010) and macrofaunal polychaetes (Soto et al., 2010) suggesting that the benthic community overall, not just megafaunal organisms, also changes significantly during such short time spans. Whilst we lack data from consecutive years at the beginning of the time series and can therefore not be sure in which specific year changes occurred, our results imply that it takes longer for large differences and separation of communities as a whole, whilst single taxa/morphotypes show significant variations in density within a one-year period. Our results also suggest that there is no “null” community, where we define a “null” community as a stable community that displays no temporal variation, as there appeared to be a constant gradually changing community at both stations. Similar to PAP there were also interannual changes in meiofaunal trophic diversities (Hoste et al., 2007; Grzelak, 2015) and bacterial community structure (Jacob, 2014) at HAUSGARTEN, particularly during the warm water period of 2005–2008 (Beszczynska-Möller et al., 2012). These two groups seem to change on different timescales however, with large changes happening over time periods less than one year. Therefore, it is unlikely that the megafaunal community, as a whole, has a large influence on or by the meiofaunal and bacterial communities. However, some megafaunal species that show significant annual changes in abundance could be influenced by/influencing the meiofaunal or bacterial communities.

Overall megafaunal densities were much higher at N3 than at S3. The most striking change in megafaunal abundance observed during the study is the three-fold increase in individuals at N3 between 2004 and 2007. This was mostly caused by an eight-fold increase in the taxonomic group “small round sponge”, as well as the deposit-feeding holothurian *Kolga hyalina*, which rose from zero to peak numbers in 2007. Large increases in deep-sea holothurian abundance and aggregation have been documented several times before, most notably with *Amperima rosea* (Billett et al., 2001) at PAP, *Elpidia glacialis* at Larsen A and B in Antarctica (Gutt et al., 2011) and *Scotoplanes globosa*, two *Peniagone* sp. and an *Elpidia* sp. at Station M, 220 km west of the central Californian coast (Kuhnz et al., 2014). These increases are usually a response to above-average, localised food input into the system leading to periods of successful and rapid breeding. Gutt (1995) showed that the ice algae *Melosira arctica* is a major contributor to the algal abundance at the subsurface of the sea ice in a nearby Arctic region and Boetius et al. (2013) found *M. arctica* in the intestines of central Arctic *Kolga hyalina* proving that the ice algae are a food source.

Surprisingly, we found no clear relationship between sea ice coverage and phytodetrital input nor between ice and megafaunal abun-

dance. Years of high ice cover did not coincide with high levels of phytodetrital matter or megafaunal density. Lalande et al. (2016) suggested that particles caught by deep sediment traps at the central HAUSGARTEN station (HG-IV; 2430 m) could have originally been produced as far as 3000 km away assuming sinking rates of 5 m d^{-1}. Lateral advection processes may thus explain the mismatch between sea ice coverage and phytodetrital matter or megafaunal density. However, this does not mean that sea-ice related algae in general do not play a role. Individuals from HAUSGARTEN station N4 (37 km north off N3, with a similar ice coverage history) contained the biomarker for ice algae, IP25 (Bergmann, unpublished data) whereas individuals from S3 did not.

Still, the initial decrease in phytodetrital matter between 2004 and 2006 matched the decrease in megafaunal abundance at S3 (this study), HG-IV and HG-I (Soltwedel et al., 2016). This was followed by a significant overall increase in phytodetrital matter after 2007, which was reflected in increased megafaunal density at all HAUSGARTEN stations (Soltwedel et al., 2016) including N3. A time lag of 0.5–1 year has been previously proposed for macro- and megafauna (Billett et al., 2010; Soto et al., 2010). This may explain, why megafaunal densities at S3 had not responded to increased food availability in 2007, with a sustained increasing trend afterwards suggesting the potentially increased carrying capacity at the site is yet to be reached. This explanation, however, contradicts the peak megafaunal abundance observed in 2007 at N3. There could be several reasons for this: (1) the megafaunal community located further North in the marginal ice zone may have reacted differently to the Atlantic warm anomaly and somehow stimulated a faster growth; (2) a strong immigration event of the slow but mobile *Kolga hyalina* has led to increased local abundance; (3) factors that were not captured by our measurements lead to increased megafaunal densities. It is clear that no single factor is the lone reason behind any of the observed variations in community structure and the megafaunal density, and further study into the life history of Arctic megafauna and continued monitoring is key into unravelling how systems that affect the communities are interlinked.

Shannon-Wiener diversity and Pielou's evenness increased over time at both stations. In most years, the communities of both stations were characterised by a higher proportion of α diversity and β diversity at an approximate 3:1 ratio of the γ diversity. However, in the years characterised by the highest γ diversity (2013, 2014) at N3 this ratio decreased to 2:1, showing that species turnover contributed more to the greater overall species richness. With an increased species richness diversity and maintenance of the 3:1 (α:β) ratio, it suggests that although the species community structure is continuously changing, the communities present are mature and well established. This is perhaps the reason why the variation in community structure observed is due to the abundances of each taxa/morphotype present, rather than which taxa/morphotypes are present.

4.2. Habitat features

Whilst the habitat features at S3 changed significantly over time, they only helped to describe the taxa/morphotypes present by a low-moderate amount. This was not the case at N3 however, where burrows and (drop-)stones strongly defined the taxa/morphotype composition present. Many burrows were observed in 2004 and were probably built by the burrowing amphipod *Neohela lamia*. Its numbers dropped sharply in 2007, and became almost absent thereafter. The stark changes seen in the almost complete terraforming of the seafloor from a burrow-dense state in 2004 to a virtually burrow-free state in 2011, and the concomitant loss of habitat heterogeneity, shows the key roles organisms can play as ecosystem engineers in controlling their environment (Buhl-Mortensen et al., 2015). The second important habitat feature for describing the community at N3 are exposed (drop-) stones. Their density remained constant every year at N3 except for 2007 where we observed a 10-fold increase. This large increase of exposed (drop-)stones may be a key driver for the large increase in megafaunal abundance and change in megafaunal community at N3. The potential impacts of higher (drop-)stone numbers could have had are: simply as hard substrata required for some organisms, elevation of suspension feeding organisms higher into the water column to allow access to a greater food opportunity due to faster currents or as potentially being used as “stepping stones”, allowing greater penetration of some taxa/morphotypes into the station, aiding with dispersal/migration (Schulz et al., 2010; Meyer et al., 2016). Meyer et al. (2016) also showed that many taxa/morphotypes at HAUSGARTEN that are associated with the (drop-)stones show significant spatial correlation, e.g. *Amphianthus* sp. and *Cladorhiza* cf. *gelida/Bathycrinus carpenterii*. Whilst a potential explanation for the 10-fold increase in (drop-) stones at N3 could be due to a slightly different sample area in 2007, the transect location data would suggest this is not the case. With the next sampled year being only 2011 it is unclear what happened to the (drop-)stones, however, the most likely explanation would be a combination of sinking into the soft sediment and sedimentation over that four-year period.

5. Conclusion

In reference to our scientific aims we were able to detect large temporal variations in megafaunal density, community structure and diversity at both the ice-influenced station N3 as well as the ice-free station S3 at HAUSGARTEN between 2004 and 2015. While there was no clear relationship with sea ice coverage, the general increase in megafaunal densities over the course of the study coincides with increased, sustained level of sediment-bound phytodetrital matter, which is probably a result of the warm anomaly observed in the region between 2005 and 2008.

It is likely that multiple further complex factors are driving the variations observed, including influences from outside the spatial scope of this study. The variations in community structure are driven by differences in the abundances of certain taxa/morphotypes, particularly those of *Neohela lamia, Kolga hyalina* and *Elpidia heckeri*, rather than the taxonomic inventory. We also conclude that the communities are constantly shifting and that no “null” community exists.

Our data highlights the importance of maintaining long term observations at HAUSGARTEN, one of the few observatories with a biological and a strong benthic component. Global coupled climate models project that we need < ca. 30 years of observations to be able to distinguish a climate change trend from natural variability in the Arctic (Henson et al., 2016) highlighting the need for sustained long-term ecological research.

Acknowledgements

We thank the officers and crew of *R/V Polarstern* for their assistance at sea during the expeditions: ARK-XX/1, ARK-XXII/1, ARK-VI/2, ARK-XXVII/2, ARK-XXVIII/1 and ARK-XXIX/2, as well as those of *R/V Maria S. Merian* during the expedition MSM29. We also thank all scientists that supervised OFOS transects, multiple corer deployments and sediment analyses. B. Sablotny provided technical support. C. Hasemann and I. Schewe were in charge of multiple corer deployment and sediment analyses assisted by A. Pappert and numerous volunteers and students.

We thank A. Vedenin (P.P. Shirshov Institute of Oceanology, RAS) for increasing our taxonomic resolution. D. Langenkämper (Universität Bielefeld) provided user support with BIIGLE, which was partly funded by the Helmholtz Alliance ROBEX (Grant no. HA-304) as was MB. JT was funded by a DAAD PhD Scholarship (Funding programme no. 57076385). This study contributes to the tasks of the Helmholtz-funded infrastructure programme FRAM (Frontiers in Arctic Marine Research). The suggestions of two anonymous reviewers improved an

earlier version of the manuscript. This publication is Eprint ID 42595 of the Alfred-Wegener-Institut, Helmholtz-Zentrum für Polar- und Meeresforschung. Supplementary data are available at https://doi.org/10.1594/PANGAEA.873000.

References

Bauerfeind, E., Nöthig, E.-M., Beszczynska, A., Fahl, K., Kaleschke, L., Kreker, K., Klages, M., Soltwedel, T., Lorenzen, C., Wegner, J., 2009. Particle sedimentation patterns in the eastern Fram Strait during 2000–2005: results from the Arctic long-term observatory HAUSGARTEN. Deep-Sea Res. I 56, 1471–1487.

Bergmann, M., Dannheim, J., Bauerfeind, E., Klages, M., 2009. Trophic relationships along a bathymetric gradient at the deep-sea observatory HAUSGARTEN. Deep-Sea Res. I 56, 408–424.

Bergmann, M., Soltwedel, T., Klages, M., 2011. Interannual dynamics of megafaunal assemblages from the Arctic deep-sea observatory, HAUSGARTEN (79°N). Deep-Sea Res. I 58, 711–723.

Beszczynska-Möller, A., Fahrbach, E., Schauer, U., Hansen, E., 2012. Variability in Atlantic water temperature and transport at the entrance to the Arctic Ocean, 1997–2010. ICES J. Mar. Sci. 69, 852–863.

Bett, B.J., Malzone, M.G., Narayanaswamy, B.E., Wigham, B.D., 2001. Temporal variability in phytodetritus and megabenthic activity at the seabed in the deep Northeast Atlantic. Prog. Oceanogr. 50, 349–368.

Billett, D.S.M., Bett, B.J., Rice, A.L., Thurston, M.H., Galéron, J., Sibuet, M., Wolff, G.A., 2001. Long-term change in the megabenthos of the Porcupine Abyssal Plain (NE Atlantic). Prog. Oceanogr. 50, 325–348.

Billett, D.S.M., Bett, B.J., Reid, W.D.K., Boorman, B., Priede, I.G., 2010. Long-term change in the abyssal NE Atlantic: the '*Amperima* Event' revisited. Deep-Sea Res. II 57, 1406–1417.

Boetius, A., Albrecht, S., Bakker, K., Bienhold, C., Felden, J., Fernandez-Mendez, M., Hendricks, S., Katlein, C., Lalande, C., Krumpen, T., Nicolaus, M., Peeken, I., Rabe, B., Rogacheva, A., Rybakova, E., Somavilla, R., Wenzhöfer, F., 2013. Export of algal biomass from melting arctic sea ice. Science 339, 1430–1432.

Buhl-Mortensen, L., Vanreusel, A., Gooday, A.J., Levin, L.A., Priede, I.G., Buhl-Mortensen, P., Gheerardyn, H., King, N.J., Raes, M., 2010. Biological structures as a source of habitat heterogeneity and biodiversity on the deep ocean margins. Mar. Ecol. 31, 21–50.

Buhl-Mortensen, L., Tandberg, A.H.S., Buhl-Mortensen, P., Gates, A.R., 2015. Behaviour and habitat of *Neohela monstrosa* (Boeck, 1861) (Amphipoda: Corophiida) in Norwegian Sea deep water. J. Nat. Hist.. http://dx.doi.org/10.1080/00222933.2015.1062152.

Clarke, K.R., Gorley, R.N., 2006. Primer v6: User Manual/Tutorial. PRIMER-E, Plymouth, 190.

Durden, J.M., Bett, B.J., Schoening, T., Morris, K.J., Nattkemper, T.W., Ruhl, H.A., 2016. Comparison of image annotation data generated by multiple investigators for benthic ecology. Mar. Ecol. Prog. Ser.. http://dx.doi.org/10.3354/meps11775.

Ezraty R., Girard-Ardhuin F., Piollé J.F., Kaleschke L., Heygster G., 2007. Arctic and Antarctic Sea Ice Concentration and Arctic Sea Ice Drift Estimated from Special Sensor Microwave Data, Département d'Océanographie Physique et Spatiale, IFREMER, Brest, France and University of Bremen, Germany, 2.1 edn., ftp://ftp.ifremer.fr/ifremer/cersat/products/gridded/psi-drift/documentation/ssmi.pdf.

FitzGeorge-Balfour, T., Billett, D.S.M., Wolff, G.A., Thompson, A., Tyler, P.A., 2010. Phytopigments as biomarkers of selectivity in abyssal holothurians; interspecific differences in response to a changing food supply. Deep-Sea Res. II 57, 1418–1428.

Forest, A., Wassmann, P., Slagstad, D., Bauerfeind, E., Nöthig, E.-M., Klages, M., 2010. Relationships between primary production and vertical particle export at the Atlantic-Arctic boundary (Fram Strait, HAUSGARTEN). Polar Biol. 33, 1733–1746.

Gooday, A.J., Levin, L.A., Aranda da Silva, A., Bett, B.J., Cowie, G.L., Dissard, D., Gage, J.D., Hughes, D.J., Jeffreys, R., Lamont, P.A., Larkin, K.E., Murty, S.J., Schumacher, S., Whitcraft, C., Woulds, C., 2009. Faunal responses to oxygen gradients on the Pakistan margin: a comparison of foraminiferans, macrofauna and megafauna. Deep Sea Res. II 56, 488–502.

Górska, B., Grzelak, K., Kotwicki, L., Hasemann, C., Schewe, I., Soltwedel, T., Wlodarska-Kowalczuk, M., 2014. Bathymetric variations in vertical distribution patterns of meiofauna in the surface sediments of the deep Arctic ocean (HAUSGARTEN, Fram Strait). Deep-Sea Res. I 91, 36–49.

Grassle, J.F., Sanders, H.L., Hessler, R.R., Rowe, G.T., McLellan, T., 1975. Pattern and zonation: a study of the bathyal megafauna using the research submersible Alvin. Deep-Sea Res. Oceanogr. Abstr. 22, 457–462.

Grzelak, K., 2015. Structural and Functional Diversity of Nematoda at the Arctic Deep-Sea Long-Term Observatory HAUSGARTEN (Fram Strait) (PhD Thesis). Institute of Oceanology Polish Academy of Sciences, Sopot, 206.

Gutt, J., 1995. The occurrence of sub-ice algal aggregations off northeast Greenland. Polar Biol. 15, 247–252.

Gutt, J., Barratt, I., Domack, E., d'Udekem d'Acoz, C., Dimmler, W., Grémare, A., Heilmayer, O., Isla, E., Janussen, D., Jorgensen, E., Kock, K.-H., Lehnert, L.S., López-Gonzáles, P., Langner, S., Linse, K., Manjón-Cabeza, M.E., Meißner, M., Montiel, A., Raes, M., Robert, H., Rose, A., Sañé Schepisi, E., Saucède, T., Scheidat, M., Schenke, H.-W., Seiler, J., Smith, C., 2011. Biodiversity change after climate-induced ice-shelf collapse in the Antarctic. Deep-Sea Res. II 58, 74–83.

Hasemann, C., Soltwedel, T., 2011. Small-scale heterogeneity in deep-sea nematode communities around biogenic structures. PLoS One 6, e29152.

Henson, S., Beaulieu, C., Lampitt, R., 2016. Observing climate change trends in ocean biogeochemistry: when and where. Glob. Change Biol. 22 (4), (doi:1561-1571. 10.1111/gcb.13152).

Hop, H., Falk-Petersen, S., Svendsen, H., Kwasniewski, S., Pavlov, V., Pavlova, O., Søreide, J.E., 2006. Physical and biological characteristics of the pelagic system across Fram Strait to Kongsfjorden. Prog. Oceanogr. 71, 182–231.

Hoste, E., Vanhovea, S., Schewe, I., Soltwedel, T., Vanreusel, A., 2007. Spatial and temporal variation in deep-sea meiofauna assemblages in the marginal ice zone of the Arctic Ocean. Deep-Sea Res. Part I: Oceanogr. Res. Pap. , 54, 109–129.

Jacob, M., 2014. Influence of Global Change on Microbial Communities in Arctic Sediments (PhD Thesis). University of Bremen, 178.

Jacob, M., Soltwedel, T., Boetius, A., Ramette, A., 2013. Biogeography of Deep-sea benthic bacteria at regional scale (LTER HAUSGARTEN, Fram Strait, Arctic). PLoS One 8, e72779.

Jones, C.G., Lawton, J.H., Shachak, M., 1994. Organisms as ecosystem engineers. OIKOS 69, 373–386.

Kalogeropoulou, V., Bett, B.J., Gooday, A.J., Lampadariou, N., Arbizu, P.M., Vanreusel, A., 2010. Temporal changes (1989–1999) in deep-sea metazoan meiofaunal assemblages on the Porcupine Abyssal Plain, NE Atlantic. Deep-Sea Res. II 57, 1383–1395.

Kauker, F., Kaminski, T., Karcher, M., Giering, R., Gerdes, R., Vossbeck, M., 2009. Adjoint analysis of the 2007 all time Arctic sea-ice minimum. Geophys. Res. Lett. 36, L03707.

Kuhnz, L.A., Ruhl, H.A., Huffard, C.L., Smith, K.L., Jr., 2014. Rapid changes and long-term cycles in the benthic megafaunal community observed over 24 years in the abyssal northeast Pacific. Prog. Oceanogr. 124, 1–11.

Lalande, C., Bauerfeind, E., Nöthig, E.-M., Beszczynska-Möller, A., 2013. Impact of a warm anomaly on export fluxes of biogenic matter in the eastern Fram Strait. Prog. Oceanogr. 109, 70–77.

Lalande, C., Nöthig, E.-M., Bauerfeind, E., Hardge, K., Beszczynska-Möller, A., Fahl, K., 2016. Lateral supply and downward export of particulate matter from upper waters to the seafloor in the deep eastern Fram Strait. Deep-Sea Res. I 114, 78–89.

Lauerman, L.M.L., Kaufmann, R.S., Smith, K.L., 1996. Distribution and abundance of epibenthic megafauna at a long time-series station in the abyssal northeast Pacific. Deep-Sea Res. I 43, 1075–1103.

MacDonald, I.R., Bluhm, B.A., Iken, K., Gagaev, S., Strong, S., 2010. Benthic macrofauna and megafauna assemblages in the Arctic deep-sea Canada Basin. Deep Sea Res. II 57 (1–2), 136–152.

Meyer, K.S., Bergmann, M., Soltwedel, T., 2013. Interannual variation in the epibenthic megafauna at the shallowest station of the HAUSGARTEN observatory (79°N, 6°E). Biogeosciences 10, 3479–3492.

Meyer, K.S., Soltwedel, T., Bergmann, M., 2014. High biodiversity on a deep-water reef in the Eastern Fram Strait. PLoS One 9, e105424.

Meyer, K.S., Young, C.M., Sweetman, A.K., Soltwedel, T., Taylor, J., Bergmann, M., 2016. Rocky islands in a sea of mud: biotic and abiotic factors structuring deep-sea dropstone communities. Mar. Ecol. Prog. Ser. 556, 45–57.

Ontrup, J., Ehnert, N., Bergmann, M., Nattkemper, T.W., 2009. Biigle – Web 2.0 enabled labelling and exploring of images from the Arctic deep-sea observatory HAUSGARTEN. In: Proceedings of OCEANS 2009 – EUROPE. Doi: 10.1109/OCEANSE.2009.5278332.

Rex, M.A., 1981. Community structure in the deep-sea benthos. Annu. Rev. Ecol. Syst. 12, 331–353.

Ruhl, H.A., 2007. Abundance and size distribution dynamics of abyssal epibenthic megafauna in the northeast Pacific. Ecology 88, 1250–1262.

Schoening, T., Bergmann, M., Ontrup, J., Taylor, J., Dannheim, J., Gutt, J., Purser, A., Nattkemper, T.W., 2012. Semi-automated image analysis for the assessment of megafaunal densities at the Arctic deep-sea observatory HAUSGARTEN. PLoS One 7, e38179.

Schoening, T., Kuhn, T., Bergmann, M., Nattkemper, T.W., 2015. Delphi - an iteratively learning laser point detection. Front. Mar. Sci. 2. http://dx.doi.org/10.3389/fmars.2015.00020.

Schulz, M., Bergmann, M., von Juterzenka, K., Soltwedel, T., 2010. Colonisation of hard substrata along a channel system in the deep Greenland Sea. Polar Biol. 33, 1359–1369.

Smith, C.R., De Leo, F.C., Bernardino, A.F., Sweetman, A.K., Arbizu, P.M., 2008. Abyssal food limitation, ecosystem structure and climate change. Trends Ecol. Evol. 9, 518–528.

Soltwedel, T., Bauerfeind, E., Bergmann, M., Bracher, A., Budaeva, N., Busch, K., Cherkasheva, A., Fahl, K., Grzelak, K., Hasemann, C., Jacob, M., Kraft, A., Lalande, C., Metfies, K., Nöthig, E.-M., Meyer, K., Quéric, N.-V., Schewe, I., Wlodarska-Kowalczuk, M., Klages, M., 2016. Natural variability or anthropogenically-induced variation? Insights from 15 years of multidisciplinary observations at the arctic marine LTER site HAUSGARTEN. Ecol. Indic. 65, 89–102.

Soto, E.H., Paterson, G.L.J., Billett, D.S.M., Hawkins, L.E., Galeron, J., Sibuet, M., 2010. Temporal variability in polychaete assemblages of the abyssal NE Atlantic Ocean. Deep-Sea Res. II 57, 1396–1405.

Spreen, G., Kaleschke, L., Heygster, G., 2008. Sea ice remote sensing using AMSR-E 89 GHz channels. J. Geophys. Res. 113, 1–14.

Taylor, J., Krumpen, T., Soltwedel, T., Gutt, J., Bergmann, M., 2016. Regional- and local-scale variations in benthic megafaunal composition at the Arctic deep-sea observatory HAUSGARTEN. Deep-Sea Res. I 108, 58–72.

Teixidó, N., Garrabou, J., Gutt, J., Arntz, W., 2004. Recovery in Antarctic benthos after iceberg disturbance: trends in benthic composition, abundance and growth forms. Mar. Ecol. Prog. Ser. 278, 1–16.

Teixidó, N., Garrabou, J., Gutt, J., Arntz, W., 2007. Iceberg disturbance and successional spatial patterns: the case of the shelf Antarctic benthic communities. Ecosystems 10 (1), 143–158.

von Appen, W.-J., Schauer, U., Somavilla Cabrillo, R., Bauerfeind, E., Beszczynska-Möller, A., 2015. Exchange of warming deep waters across Fram Strait. Deep-Sea Res. I 103, 86–100.

Wang, M., Overland, J.E., 2009. A sea ice free summer Arctic within 30 years? Geophys. Res. Lett. 36 (7), L07502.